Semi-static Object Detection using Polygonal Maps for Safe Navigation of Industrial Robots

Dario Lodi Rizzini, Gionata Boccalini and Stefano Caselli
Dipartimento di Ingegneria dell'Informazione, University of Parma, viale G.P. Usberti 181A, 43124 Parma, Italy

Keywords: Mapping, Range Sensing.

Abstract: The collision and safety control of industrial UGVs equipped with laser range finders is often based on conservative area-oriented policies that lack in flexibility and does not deal well with non ephemeral environment changes due to semi-static objects (e.g. passive misplaced objects). In this paper, we propose a method to detect and represent semi-static objects using polygonal local maps in order to improve robot navigation. Each local map consists of polylines representing the boundary of an object detected inside a safety area. Polylines are extracted from laser scans and associated with the polylines of a reference map using a similarity measure criterion. Finally, the map is updated by merging the new polylines. The proposed polygonal representation allows the recognition of new semi-static obstacles in the environment and supports more flexible policies for safe navigation. An EKF localizer using artificial landmarks and a fixed path navigation system have been implemented to replicate the navigation system of industrial UGVs. The precision of environment reconstruction has been assessed with experiments in simulated and real environments.

1 INTRODUCTION

Unmanned Ground Vehicles (UGVs) are more and more used to manage logistics, individually or in coordinated teams, in industrial plants and warehouses. Being completely autonomous, these vehicles are usually equipped with laser range finders to perceive obstacles and to localize and navigate in the environment. Laser range finders for localization are usually mounted on the LGV top to avoid occlusions and to perceive artificial landmarks with high remission value that have been previously placed in the environment. An Extented Kalman Filter (EKF) localizer tracks and estimates the pose of the robot using the observed landmarks and an a priori map of the landmarks. Safety lasers (e.g. Sick S300) are usually placed slightly above floor level for the detection of any object lying in the proximity of the robot. One common safety policy consists of partitioning the space in front of the laser *idle*, *warning* and *protective* areas. The warning and the protective areas are supposed to be free in normal working conditions so an appropriate size for the areas must be defined for each segment of the LGV trajectory. When an object is perceived in the warning area (shown in yellow in bottom of Figure 1), the UGV slows down according to the warning. When the protective area (in red in Figure 1) is not free, the vehicle stops. For any plant operating with LGVs, the dimensions of warning and protective areas vary in the different regions of the working environment. This strict and conservative policy grants the safety of people and things, but it is inefficient and inflexible. Sizing the safety areas is a time-consuming and tedious operation that must be repeated whenever the environment layout changes. Furthermore, while it is mandatory that the robot stops when a collision with a person or an obstacle may occur, the efficiency of the system is often affected by objects thoughtlessly left in the assumed free space. Although the area classification scheme has been conceived to ensure safety margin in presence of human operators, the majority of reduction in UGV navigation speed is actually due to passive misplaced objects. These objects may be modeled as *semi-static objects* that do not belong to the persistent structure of the environment. Semi-static objects change their location with low frequency (e.g. after several hours) and while the robot is not observing them.

In this paper, we propose a method to detect and represent semi-static objects using polygonal local maps in order to improve robot navigation. In the proposed solution, the representation of semi-static objects is assigned to a collection of local maps where each local map covers a specific path segment. Local maps are more manageable than a single global map and can be more easily integrated with the existent

Lodi Rizzini D., Boccalini G. and Caselli S..
Semi-static Object Detection using Polygonal Maps for Safe Navigation of Industrial Robots.
DOI: 10.5220/0003989601910198
In *Proceedings of the 9th International Conference on Informatics in Control, Automation and Robotics* (ICINCO-2012), pages 191-198
ISBN: 978-989-8565-22-8

navigation system. Such maps consist of polygonal lines or, shortly, *polylines* that represent the boundary of the obstacles found inside the warning and protective areas. Polygonal representation is memory and bandwidth inexpensive, compact and semantically rich. A similarity measure is used to associate the observed polylines with a preexisting map for robust detection of semi-static objects. When a semi-static object is found inside a safety area, the corresponding local map is updated and the dimension of the safety areas of the laser range sensor may be adapted to the reduced free space. Thus, the next LGV visiting the same region is not forced to slow down or to stop since the updated area does not contain semi-static object. More advanced and efficient policies may be implemented by giving up the conservative safety area. The proposed approach has been assessed in simulation and in a real experimental setup. For this purpose, an EKF localizer based on landmark and a navigation system have been implemented.

2 RELATED WORK

Research on robot localization and map building early met the problem of representing dynamics in the environment. The first and most common approach is the removal of moving objects when detected. Fox *et al.* (Fox et al., 1999) proposed a sensor model for range finders that can deal with dynamic objects by modeling them as noise. The work of Wolf *et al.* (Wolf and Sukhatme, 2005) is one of the first simultaneous localization and mapping (SLAM) methods that explicitly distinguishes between dynamic entities and static environments using two different occupancy grid maps. Stachniss *et al.* (Stachniss and Burgard, 2005) focus on the semi-static objects, i.e. objects that infrequently change their location while the robot is not observing them. Semi-static objects like doors, parking locations, etc., often define the discrete state of the environment providing also long-term semantic information. Recent localization methods represent static, semi-static and dynamic objects in the map (Meyer-Delius et al., 2010). The majority of these techniques are based on an occupancy grid map, which is suitable to integrate range measurements into a robust representation of the environment, but it does not carry shape or semantic information (an object corresponds to a group of cells) and is not apt to be shared among distributed robots.

Several other works identifies either generic (Katz et al., 2008) or specific moving entities like people (Spinello et al., 2009) from consecutive range measurements. Tipaldi and Ramos (Tipaldi and Ramos, 2009) proposed a method performing simultaneously scan matching and moving cluster detection using Conditional Random Fields (CRF). These approaches are oriented only to the detection and short-term tracking of people and objects and represent their targets as clusters of points.

Strict-sense polygonal representations have not been extensively used for mapping, since a polyline is a composite element and cannot be represented with a fixed number of variables as would be convenient for state estimation algorithms like Bayesian filters. On the other hand, EKF localization and mapping algorithms often utilize line segment feature maps according to models like SP-map models (Arras, 2003). Latecky *et al.* (Latecki et al., 2004) illustrated a techniques for integrating the polylines extracted by range measurements by exploiting shape similarity measure and scan order.

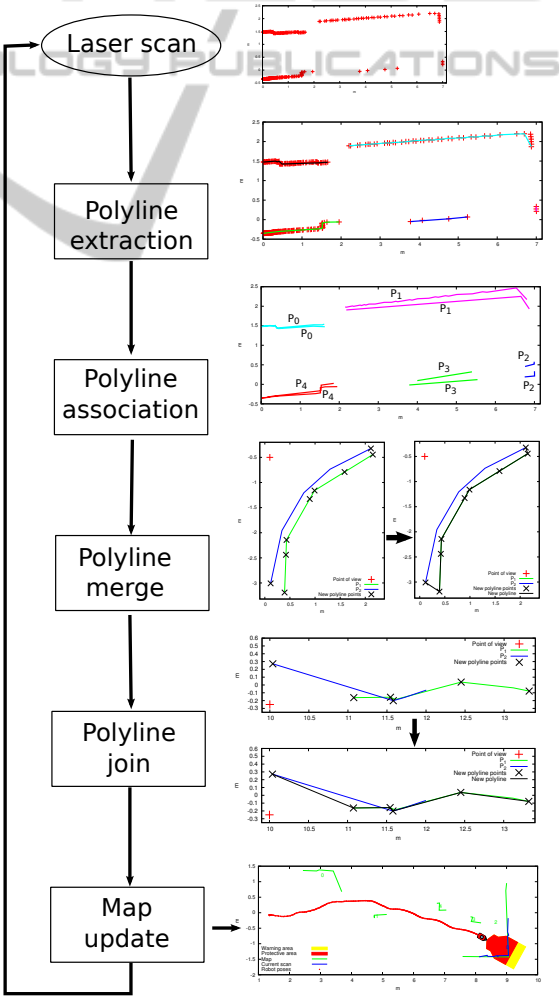

Figure 1: Diagram illustrating the algorithm for building polygonal maps from laser scans.

3 POLYGONAL MAP REPRESENTATION

This work aims to detect and track the non ephemeral changes occurring inside the region of environment covered by the robot range sensors. The robot moves along a collection of path segments defined a priori. On each path segment a specific safety area (consisting of warning and protective areas) is defined to detect potential obstacles without including the static part of environment. When a stationary entity is detected inside a safety area, the system should record such semi-static object in a map of the environment. Instead of managing a single global map, the natural segmentation of the robot path can be exploited to cover the working environment with more manageable local maps of limited dimensions. The reference frames of these local maps are anchored to the reference frame on the path segments.

A local map consists of polygonal lines or polylines that are represented by the list of their vertices. Polylines are compact geometric features that represent the countour of obstacles and that can be easily extracted by laser range scans. Polygonal maps meet several of the system requirements. First, polylines require limited storage and bandwidth for their transmission among the LGVs working together in the environment. Second, the result of polylines extraction from laser scan is already a segmented set since each polyline represents an object or a portion of an object, though the extraction algorithm must handle errors due to occlusions and sensor noise. Finally, polylines encode shape information that would be implicit in occupancy grid representations and that can be exploited for robust data association.

The steps of the algorithm for extracting and integrating the polylines from the laser scan into a consistent map are illustrated in Figure 1. The algorithm extracts polylines from current laser scan (polyline extraction) and associates them with the polylines contained in the existing map using the similarity measure (polyline association). Then, the scan polylines are merged with the associated elements of the map (polyline merge). Finally, the close polygonal lines are joined to remove inconsistent and redundant items (polyline join). In the following, the details of the proposed algorithm are discussed.

3.1 Polyline Extraction

Polylines are extracted from each raw laser range scan by removing outliers, by splitting the scan into intervals and finally by choosing the vertices of the polylines. Scans are commonly represented as sorted vectors of ranges or, equivalently, of points (symbols r_i and p_i will refer to range or Cartesian point hence after). The implicit angular order of ranges is used by the standard extraction techniques (Xavier et al., 2005) as those applied in this work.

First processing step is the statistical outlier removal. For each window of ranges $r_{i-k}, \ldots, r_i, \ldots, r_{i+k}$ centered on $i-th$ range the mean value μ_i and standard deviation σ_i are computed. The two statistics are used to detect isolated measurements. If the difference between range r_i and window mean value μ_i is greater than a threshold $\alpha\ \sigma_i$ (α is a parameters set by the user), then measurement i is removed from the scan. The scan is then split into intervals in correspondence to a strong discontinuity between consecutive ranges. The discontinuity is detected according to the standard adaptive threshold criterion. The line connecting two consecutive discontinuous points represents the border of the occluded region.

Each scan interval corresponds to a polyline representing an object or a part of an object. All the points of an interval may serve as vertices of the polyline. However, when points are approximatively aligned, the polyline is better represented by a less redundant list of points. Such result can be easily achieved using Douglas-Peuker algorithm for curve simplification (Douglas and Peuker, 1973). A similar result could be obtained using the *discrete curve evolution* (DCE) proposed in (Latecki et al., 2004).

3.2 Metric for Polylines

The association of polylines belonging to different sets is a crucial operation for the construction of local map and for the detection of the objects that have been already observed or not yet observed. Association is performed on two sets of polylines, i.e. the polylines extracted from the laser scan and the polylines belonging to the existing local map. Polyline association requires a metric to measure the likeness of a single pair of polylines and a procedure to estimate the most consistent joint set of associated pairs. The latter aspect is discussed in the next section.

In this work, two different metrics are used. The first one aims at measuring the shape *similarity* between two polylines. The second estimates a bound on the Euclidean distance between the points of two polylines to validate the similarity. Since the robot pose can be accurately estimated using a localizer, the pose of polylines in the map is accurate enough to use proximity as a validation of data association.

Two simple curves in the plane are perceived as similar if their tangent vector "turns" in the same way.

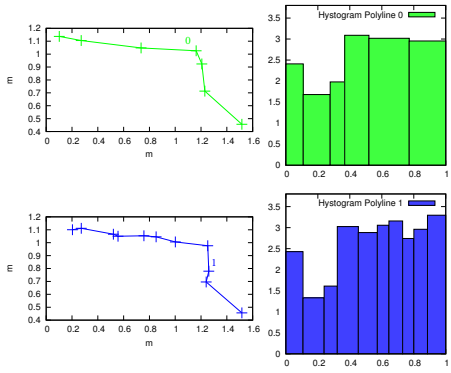

Figure 2: Polyline shape similarity of polyline 0 (top-left) and polyline 1 (bottom-left) is measured comparing their respective tangent space histograms (top- and bottom-right).

The concept of similarity has been originally formalized in (Latecki and Lakaemper, 1999) for closed polygons and then extended to polylines (Latecki et al., 2004). The idea is to compare the normalized tangent histograms of two polylines P_0 and P_1. The polygonal curves $P_0 s$ and $P_1 s$ are parameterized w.r.t. their normalized arclength $s \in [0,1]$. The tangent function $T_{P_0}(s) : [0,1] \mapsto [0,2\pi]$ (and $T_{P_1}(s)$) returns the angle between the axis x and the tangent vector to the polyline in $P_0(s)$ (and $P_1(s)$). Since the polyline consists of edges and the tangent angle on each edge is constant, the tangent space function has the appearance of a histogram. Figure 2 illustrates the normalized tangent space histograms of two different polylines. Tangent histogram is invariant to translation and a rotation applied to a polyline shifts up or down all the values of the corresponding tangent histogram, but the difference between tangent angles remains invariant. Furthermore, tangent histogram is not affected by the scale of the polylines since it is parameterized w.r.t. the normalized arc length. Thus, tangent histograms can be used to define a metric that is invariant to both rigid motion and scale. Similarity measure $S(P_0,P_1)$ of polylines P_0 and P_1 is formally defined by equation

$$s(P_0,P_1) = \int_0^1 (T_{P_1}(s) - T_{P_0}(s) + \theta_0)^2 ds \max\left[\frac{l_1}{l_0}, \frac{l_0}{l_1}\right] \quad (1)$$

$$\theta_0 = \int_0^1 (T_{P_1}(s) - T_{P_0}(s))\, ds \quad (2)$$

where l_0 and l_1 are the lengths respectively of the polygons P_0 and P_1 and θ_0 is the angle that minimizes the mean difference between the histograms. The second term of equation (1) is introduced to weight the length of the polylines in the similarity that would be otherwise invariant to scale. The above integral is concretely computed on a refinement of the arclength intervals.

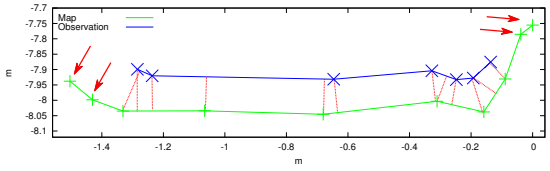

Figure 3: An example of the computation of restricted polylines $P_0|_{P_1}$ and $P_1|_{P_0}$: the red arrows point out the vertices of P_0 not belonging to $P_0|_{P_1}$.

The invariance of similarity measure is clearly an advantage beacuse repeated observations of the same object are seldom gathered from the same point of view. However, if the object shape is ambigous or not enough distinctive, similarity measure may be misleading. The association procedure defined in the following may attenuate such problem, but a validation of similarity that takes into account the distance between polylines should be performed through a proper metric. Hausdorff distance provides a worst case estimate of the distance between two polylines P_0 and P_1 and is often used to compute the distance between two composite geometric sets. When two polylines represent the same object and one of them is obtained from a partial view of the object, the Hausdorff distance may overestimate the Euclidean displacement between the polylines. To overcome this inconvenience we define a metric that compares the distance of two polylines restricted to the overlapping part. The definition is based on the correspondence between the index order of vertices and the angular order of the original laser scan points that remain in the polylines also after several merges. Let P_0 and P_1 be two polylines respectively with vertices $p_{0,0}, p_{0,1}, \ldots, p_{0,n_0-1}$ and $p_{1,0}, p_{1,1}, \ldots, p_{1,n_1-1}$. Let ${}^0_1 i_k$ be the index of the segment of P_0 closer to vertex $p_{1,k}$ of polygon P_1 or, formally,

$${}^0_1 i_k \triangleq \underset{j=1,\ldots,n_0-1}{\operatorname{argmin}} \; \mathrm{d}(p_{1,k}; \overline{p_{0,j-1} p_{0,j}}) \quad (3)$$

The minimum and maximum indices are defined as follows ${}^0_1 i_{min} = \min\{{}^0_1 i_0, \ldots, {}^0_1 i_{n_1}\}$ and ${}^0_1 i_{max} = \max\{{}^0_1 i_0, \ldots, {}^0_1 i_{n_1}\}$. Thus, the polyline $P_0|_{P_1}$ restricted to P_1 consists of the vertices p_{0i} with $i = {}^0_1 i_{min}, \ldots, {}^0_1 i_{max}$. Similarly, we define the polyline $P_1|_{P_0}$ restricted to P_0. Figure 3 illustrates the effect of restriction on polylines. Thus, the *restricted Hausdorff distance* is defined as the Hausdorff distance of the restricted polylines and can be used to limit the risk of misleading estimations.

3.3 Polyline Association

The metrics defined in the previous section can be

used to associate the polylines extracted from the scan with the polylines contained in the existing local map. The natural order of the polylines in the laser scan can be exploited to reduce the risk of wrong association. Map polylines can also be dynamically sorted according to the current viewpoint of the robot. Such constrained order also reduces the complexity of data association problem and that be solved using dynamic programming optimization as suggested in (Latecki et al., 2004). Let $\mathcal{S}_i = \{S_0, S_1, \ldots, S_i\}$ be the sorted list of the scan polylines from the first to the $i-th$ $(i = 0, \ldots, n)$ and $\mathcal{M}_j = \{M_0, M_1, \ldots, M_j\}$ be the sorted list of the map polylines till the $j-th$ $(j = 0, \ldots, m)$. The solution of polyline association problem restricted to $\mathcal{S}_i$ and $\mathcal{M}_j$ is given by the sorted list of index pairs $\mathcal{A}_{ij}$ and the total distance between the associated polylines is

$$d(\mathcal{A}_{ij}) = \sum_{(\bar{i},\bar{j})\in\mathcal{A}_{ij}} s(S_{\bar{i}}, M_{\bar{j}}) \tag{4}$$

where $s(\cdot)$ is the similarity measure of polylines discussed in previous section. The solution $\mathcal{A}_{ij}$ is the list of pairs that minimizes the distance of equation (4) of the restricted problem. Given two distinct association pairs $(i_1, j_1), (i_2, j_2) \in \mathcal{A}_{ij}$ the strict condition $i_1 \leq i_2$ and $j_1 \leq j_2$, briefly $(i_1, j_1) < (i_2, j_2)$, must hold (without loosing generality, otherwise swap i_1 with i_2 and j_1 with j_2). Hence, the best association $\mathcal{A}_{ij}$ can be estimated considering the solution of sub-problems $\mathcal{A}_{i-1,j}$, $\mathcal{A}_{i,j-1}$ and $\mathcal{A}_{i-1,j-1}$. In particular, the total distance of the solution is such that

$$\mathcal{A}_{ij} = \{(i,j)\} \cup \underset{\mathcal{A}_{i-1,j};\mathcal{A}_{i,j-1};\mathcal{A}_{i-1,j-1}}{\operatorname{argmin}} d(\mathcal{A}) \tag{5}$$

Observe that according to the above definition $\mathcal{A}_{ij}$ contains many-to-many associations. The procedure is iterated until the final association set $\mathcal{A}_{nm}$ is achieved. Since at each iteration a new pairs is inserted according to equation (5), the final set contains pairs that have been forcibly included in spite of their similarity. Thus, the restricted Hausdorff distance can be used to validate the associations contained in $\mathcal{A}_{nm}$ by fixing a threshold on the maximum distance.

3.4 Merging Polylines in the Map

Once the polylines from the scan are associated to the the polylines in the map, the map is updated by merging the associated polygonal items and by inserting the unassociated ones. The counterclockwise scan order around the viewpoint discussed previously is also exploited to merge the polylines. The polylines directly extracted from a scan are already sorted and the map polylines are sorted counterclockwise w.r.t. the current viewpoint. Our algorithm for polyline merging scans the two sorted lists, while keeping the pointer P_0 to the current map polyline aligned with the current scan polyline P_1. When P_0 and P_1 overlap, the vertices of polyline P_1 are projected on P_0 (i.e. on the map) and the resulting merg polyline is smoothed using Douglas-Peucker algorithm. Otherwise, P_0 and P_1 are respectively kept or added to the map.

The previously illustrated union of polylines produces a new collection of polylines from the old local map and the features extracted from the scan. The new map may contains overlapping polylines or small inconsistencies caused by partial views of the same object and by inaccuracies in polygon extraction. To correct such faults and to reduce the size of the map, such polylines are joined together. First, the polylines are sorted once again according to the same scan viewpoint order to detect overlapping parts through a linear scan of the polylines list. The overlapping items are found using the restricted Hausdorff distance. Second, the joining method is similar to the merging algorithm is applied.

4 SEMI-STATIC MAPS

The algorithm described in the previous section can be used to build a polygonal map from a sequence of laser scans. For each path segment, the robot keeps a local map consisting of polylines that contains the objects found inside the safety areas. Since the aim of this work is to improve area based policies for industrial environments, only the polylines that intersect the safety areas are considered. Furthermore, the proposed technique takes care of merging and joining overlapping polylines. Thus, we can assume that each polyline represents a distinguishable semi-static object of the environment.

Every time an UGV visits a region of the environment, polylines are extracted from each scan and associated with the polylines of the local map corresponding to this region. The data association technique described in section 3.3 is crucial for the detection of environmental changes. In particular, the similarity measure and the scan order help to identify the candidate association pairs and the reduced Hausdorff distance is used for the validation according to a validation gate criterion. The results presented in section 6 show that a convenient acceptance threshold for our experimental setup is slightly above 10 cm. The unassociated scan polylines are classified as new semi-static objects and inserted into the local map. The unassociated polylines in the map are marked as blank and removed after they have not been not observed for k times.

The simple semi-static map can be used to define new navigation policies. In particular, when semi-static obstacles are detected, the system can reduce one or both the safety areas (the warning and protective areas) for the path segments so that no obstacle lies inside these maps. A less conservative and more flexible rule could compare the polylines without regard to the areas and classify the obstacle as an already observed obstacle that can be ignored. However, the aim of this work is not to define a policy, but to provide the means for efficiently dealing with non static environments to the developers of the navigation system.

5 LOCALIZATION AND NAVIGATION

5.1 EKF Localization

The standard localization system of industrial LGVs works with artificial landmarks that can easily detected by laser range scanners due to the remission value of landmark material. Localization is fundamental to perform robot navigation and also to build the local maps as illustrated in section 3. Navigation based on path following requires an accurate measure of pose displacement between the current and the desired pose to perform the proper correction as will be discussed in the next subsection. A correct estimate of robot pose allows consistent positioning of the polylines in the local map.

This work aims at assessing the viability and effectiveness of semi-static object detection in the working condition of industrial mobile robots. For this purpose, a localization system based on artificial landmarks has been setup in our laboratory. Artificial landarks have been placed in the environment as shown in Figure 4(a)-(c) and a map containing the position of landmarks is available. The details of the experimental setup will be described in section 6. Given the approximate information about the group of markers visibile at the robot location, a triangulation algorithm (Esteves et al., 2003) provides the initial estimate of the robot pose. The algorithm requires three visible landmarks to provide the estimate of pose since it belongs to the category of *three object triangulation* methods. The triangulation also returns the estimation of covariance matrix representing the uncertainty on pose.

The *Extended Kalman Filter* (EKF) is the core component of the localizer and has the responsibility of keeping updated the estimate of the robot pose. The EKF uses a prediction model based on reference frame transformation rather than a velocity model and a point-landmark sensor model. In our setup, an iteration of EKF including prediction and correction is performed in about 40 *ms* and is rather efficient.

The state of the localizer representing the robot pose is referred to a unique global reference system instead of the local map frame. Currently, the localizer is completely independent from the map building component. Such solution is convenient since it does not interfere with the preexistent localization system. In future works, the polygonal features of the local map could be used by the EKF within the artificial markers, e.g. adopting an extended SP-map model (Arras, 2003).

5.2 Navigation

A complete navigation system like those described in the introduction works at different level from the path planning to reach specific goals. Our aim is only to partially reproduce the portion of the system required to build a local map. To this purpose the robot moves on a fixed path consisting of connected third order splines so that the complete path is continuous and smooth. Figure 4(right) shows an example of path represented by a red line. The path following algorithm used in this paper is the classical chained-form controller for unicycle robots (Morin and Samson, 2008). The controller require an estimate of the position and orientation errors x_e, y_e and θ_e expressed in the robot reference frame. Given the reference values of linear and angular velocities, respectively $u_{r,1}$ and $u_{r,2}$, the control equations are given by

$$\begin{cases} u_1 = u_{1,r} - K_1 \left| u_{1,r} \right| x_e \\ u_2 = u_{2,r} - K_2 \, u_{1,r} \, y_e - K_3 \left| u_{1,r} \right| \tan \theta_e \end{cases} \quad (6)$$

In our experiments we use the following values of control parameters $K_1 = 3$, $K_2 = 1.5$ and $K_3 = 1.5$.

6 RESULTS

The proposed method for building semi-static maps has been assessed using both simulation data and experiments in the real environment. The tests have been performed in two simulated environments (*Sim1* and *Sim2*) and in the hallways of building 1 (*Pal1*) and building 3 (*Pal3*) of the Computer Engineering Department of the University of Parma. In environment *Pal3* two experiments have been executed that are labeled respectively as *Pal3a* and *Pal3b*. In the latter experiments, a person moved in front of the robot to assess how small objects affect the map. The results

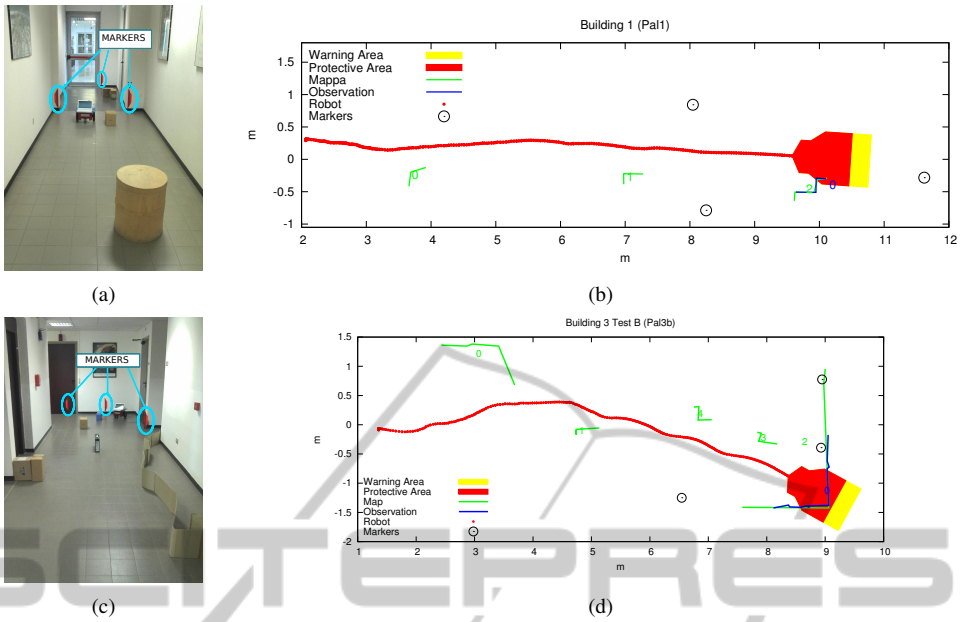

Figure 4: Pictures of experimental environments in Building 1 (*Pal1*) (a) and Building 3 (*Pal3* (c) and the respective polygonal maps (b) and (d).

shown in the following are not significantly different from those achieved in other environments, even without a specific filter for dynamic objects. Simulations have been performed using the *MobileSim* simulator provided within the MobileRobots ARIA library that introduces noise both to odometry and range finder measurements, although not controlled by the user. Real experiments have been executed on a MobileRobots *Pioneer 3DX* equipped with a Sick LMS100 laser scanner. Figures 4(a)-(c) illustrate the real environments Pal1 and Pal3.

In each environment, the robot repeatedly moved on a fixed path consisting of the union of third order splines. The length of the path is approximatively $9-12$ *m* in each test run. Obstacles have been placed so that, while the robot moves along its trajectory, such objects partially or totally lie inside the warning or the protective areas. The measurements collected during the first transit of the robot are used to build the local map of each environment that is used as reference map for the successive acquisitions. During each next transit, the robot extracts polylines from each laser scan and associates them to the corresponding polylines of the reference map according to the proposed algorithm. The new polylines are not merged into the reference map since the purpose of the experiment is the assessment of the proposed representation. Figures 4(b)-(d) illustrate the polygonal maps obtained in the experimental tests Pal1 and Pal3b.

In the simulation tests, the robot pose has been estimated only by integrating odometry information

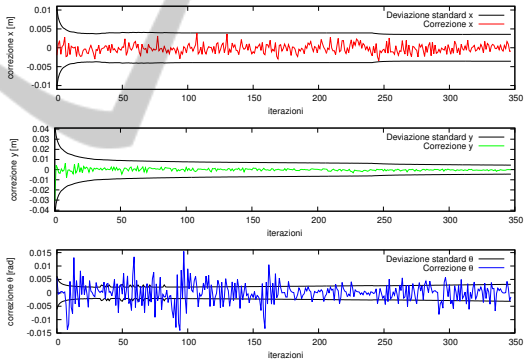

Figure 5: Corrections performed by the EKF localizer on state variables x, y and θ during an experiment.

Table 1: Average, minimum and maximum restricted Hausdorff distances of the polylines w.r.t. reference maps within the respective standard deviation for each simulated and real environment.

Environment	Distance [cm]					
	Mean			Std Dev		
	Avg	Min	Max	Avg	Min	Max
Sim1	4.71	2.19	6.62	1.89	1.25	2.69
Sim2	4.46	1.20	12.37	2.13	0.91	5.14
Pal1	2.46	1.78	2.86	1.09	0.99	1.16
Pal3a	3.99	2.14	5.94	1.68	0.70	3.18
Pal3b	4.55	2.88	6.86	1.72	1.21	3.45

due to the limitations of the simulator. In particular, the simulated groundtruth is not directly accessible by the application and the laser data do not include the beam remission values making impossible to detect reflective markers. Thus, the EKF localizer described

in section 5 can be used only for tests in real environment. Figure 5 illustrates the trend of the correction performed by the EKF filter on robot state variables x, y and θ for a single test run in *Pal1* within the corresponding σ-bound computed from the covariance matrix. The value of correction is bound by or comparable to the σ-bound. Similar measures have been performed in all the runs and for all the environments. In all cases, the standard deviation is less than 6 *mm* for position and 0.020 *rad* for angular variables.

The precision of the polygonal maps is measured by the restricted Hausdorff distances between the corresponding polylines of the reference map and of current observation. Table 1 reports the results for the different environments. For each polyline i of the reference map, the mean restricted Hausdorff distance μ_i and the corresponding standard deviations σ_i have been estimated. The results in the table are respectively the average, minimum and maximum values of mean distances μ_i and standard deviations σ_i for all the polylines. The mean distance and variance in the simulated environments are greater than in the real environments. This outcome can be explained with the high accuracy achieved by the localizer. The overall error is always less than 10 *cm*.

7 CONCLUSIONS

In this paper, we have presented a method to build polygonal local maps that manage semi-static objects in order to improve the navigation of industrial UGVs. The maps consists of polylines extracted from laser scans representing the boundary of objects. The proposed methods extracts, associates and merges the polylines obtained from the scan into a consistent map. The proposed data association algorithm is based on both the shape similarity measure and the restricted Hausdorff distance, a novel metric proposed in this work. The accurate environment reconstruction allows the identification of semi-static objects and the definition of efficient navigation policies. To replicate the navigation system of industrial UGVs, an EKF localizer and a fixed path navigation system have been implemented. Experimental results show that the error of the reconstruction is smaller than 10 *cm*. In our future works, we expect to exploit the polygonal into a complete localization and mapping algorithm.

ACKNOWLEDGEMENTS

This research is partially supported by SICK SPA.

REFERENCES

Arras, K. O. (2003). *Feature-Based Robot Navigation in Known and Unknown Environments*. PhD thesis, Swiss Federal Institute of Technology Lausanne (EPFL), Thèse No. 2765.

Douglas, D. and Peuker, T. (1973). Algorithms for the reduction of the number of points required to represent a digitized line or its caricature. *Cartographica: Int. Jour. for Geographic Information and Geovisualization*, 10(2):112–122.

Esteves, J. S., Carvalho, A., and Couto, C. (2003). Generalized geometric triangulation algorithm for mobile robot absolute self-localization. In *Proc. of IEEE International Symposium On Industrial Electronics (ISIE)*.

Fox, D., Burgard, W., and Thrun, S. (1999). Markov localization for mobile robots in dynamic environments. *Journal of Artificial Intelligence Research*, 11:391–427.

Katz, R., Douillard, B., Nieto, J., and Nebot, E. (2008). A self-supervised architecture for moving obstacles classification. In *Proc. of the IEEE/RSJ Int. Conf. on Intelligent Robots and Systems (IROS)*.

Latecki, L. and Lakaemper, R. (1999). Convexity rule for shape decomposition based on discrete contour evolution. *Computer Vision and Image Understanding*, 73(3):441–454.

Latecki, L., Lakaemper, R., Sun, X., and Wolter, D. (2004). Building polygonal maps from laser range data. In *ECAI Int. Cognitive Robotics Workshop*.

Meyer-Delius, D., Hess, Grisetti, G., and Burgard, W. (2010). Temporary maps for robust localization in semi-static environments. In *Proc. of the IEEE/RSJ Int. Conf. on Intelligent Robots and Systems (IROS)*, Taipei, Taiwan.

Morin, P. and Samson, C. (2008). Motion control of wheeled mobile robots. In Siciliano, B. and Khatib, O., editors, *Springer Handbook of Robotics*, pages 799–826. Springer Berlin Heidelberg.

Spinello, L., Triebel, R., and Siegwart, R. (2009). Multiclass multimodal detection and tracking in urban environments. In *Proc. of The 7th International Conference on Field and Service Robotics (FSR)*.

Stachniss, C. and Burgard, W. (2005). Mobile Robot Mapping and Localization in Non-Static Environments. In *Proc. of the National Conference on Artificial Intelligence (AAAI)*.

Tipaldi, G. and Ramos, F. (2009). Motion clustering and estimation with conditional random fields. In *Proc. of the IEEE/RSJ Int. Conf. on Intelligent Robots and Systems (IROS)*.

Wolf, D. and Sukhatme, G. (2005). Mobile robot simultaneous localization and mapping in dynamic environments. *Journal of Autonomous Robots*, 19:53–65.

Xavier, J., Pacheco, M., Castro, D., and Ruano, A. (2005). Fast line, arc/circle and leg detection from laser scan data in a player driver. In *Proc. of the IEEE Int. Conf. on Robotics & Automation (ICRA)*.